



# *Pseudomonas stutzeri* PM101005 inhaled with atmospheric particulate matter induces lung damage through inflammatory responses

Yu-Jin Jeong<sup>a,1</sup>, Chang-Ung Kim<sup>c,1</sup>, Kyung-Soo Lee<sup>a,b</sup>, Ji Hyung Kim<sup>d</sup>, Seo Young Park<sup>a</sup>, Ahn Young Jeong<sup>b,c</sup>, Jun Bong Lee<sup>e</sup>, Doo-Jin Kim<sup>b,c</sup>, Young-Jun Park<sup>a,b</sup>, Moo-Seung Lee<sup>a,b,\*</sup>

<sup>a</sup> Environmental Diseases Research Center, Korea Research Institute of Bioscience & Biotechnology (KRIBB), 125 Gwahak-ro, Daejeon, 34141, Republic of Korea

<sup>b</sup> Department of Biomolecular Science, KRIBB School of Bioscience, Korea University of Science and Technology (UST), 127 Gajeong-ro, Yuseong-gu, Daejeon, 34113, Republic of Korea

<sup>c</sup> Infectious Disease Research Center, Korea Research Institute of Bioscience & Biotechnology (KRIBB), 125 Gwahak-ro, Daejeon, 34141, Republic of Korea

<sup>d</sup> Department of Food Science and Biotechnology, Gachon University, Seongnam, 13120, Republic of Korea

<sup>e</sup> College of Veterinary Medicine & Institute of Veterinary Science, Kangwon National University, Chuncheon, Kangwon, 24341, Republic of Korea

## ARTICLE INFO

### Keywords:

Particulate matter  
Respiratory diseases  
Lungs  
*Pseudomonas stutzeri*  
Inflammatory response

## ABSTRACT

Atmospheric particulate matter (PM) contains a mixture of chemical and biological elements that pose threat to human health by increasing susceptibility to respiratory diseases. Although the identification of the microorganisms composing the PM has been assessed, their immunological impacts are still questionable. Here, we examined the mechanisms responsible for the pathogenicity of *Pseudomonas stutzeri* PM101005 (PMPS), a bacterium isolated from fine dust, in lung epithelial cells, alveolar cells, and macrophages. Relative to its comparative strain *Pseudomonas stutzeri* (PS), infections with PMPS induced higher production of inflammatory cytokines and chemokines, mediated by the activation of NF- $\kappa$ B and MAPK signaling pathways. Additionally, with three-dimensional (3D) airway spheroids which mimic the human bronchial epithelium, we confirmed that PMPS infections lead to relatively higher induction of pro-inflammatory cytokines than PM infections. Consistent results were observed in murine models as the infections with PMPS provoked greater inflammatory responses than the infections with PS. These PMPS-induced responses were mediated by the signaling pathways of the Toll-like receptors (TLRs), which regulated PMPS infection and played an important role in the expression of the antibiotic peptide  $\beta$ -defensin 3 (BD3) that suppressed PMPS proliferation. Moreover, PM pretreatment enhanced inflammatory responses and tissue damage of PMPS, while reducing BD3 expression. Overall, these results indicate that PM-isolated PMPS induce TLR-mediated inflammatory responses in lung tissues, and contributes to the understanding of the etiology of PM-induced respiratory damage.

## 1. Introduction

The devastating impact of air pollution on both the environment and human health has been perceived as a major consideration over the years (Heroux et al., 2015). Among the various air pollutants, concerns about particulate matter (PM) as a primary pollutant are pervasive worldwide, as it is accountable for the deterioration in morbidity and mortality (Brook et al. 2010; Tarin-Carrasco et al. 2021). PM is a complex mixture of chemical and biological elements of varying size and shape (Kim et al., 2020). This aerosol particle also contains several microorganisms, including bacteria, eukaryotes, archaea, and viruses

(Grahame and Schlesinger, 2005; Schlesinger and Cassee, 2003), although most of them in the inhaled PM are soil-associated and non-pathogenic (Cao et al., 2014). Yet, some of these microorganisms in PM, such as *Streptococcus pneumoniae*, *Aspergillus fumigatus*, and human adenovirus C, are pathogenic, causing allergies and respiratory diseases (Mushtaq et al., 2011; Nozza et al., 2021; Priyamvada et al., 2017). Most studies on the bacterial communities present with PM are mainly focused on bacterial diversity, including the identification of isolates (Qin et al., 2020; Yan et al., 2018). Epidemiological studies have revealed a strong correlation between exposure to fine dust and respiratory infections caused by pathogenic microorganisms (Cheng et al.,

\* Corresponding author. Environmental Diseases Research Center, Korea Research Institute of Bioscience & Biotechnology (KRIBB), 125 Gwahak-ro, Daejeon, 34141, Republic of Korea.

E-mail address: [msl031000@kribb.re.kr](mailto:msl031000@kribb.re.kr) (M.-S. Lee).

<sup>1</sup> These authors contributed equally to this work.

<https://doi.org/10.1016/j.envpol.2022.120741>

Received 13 September 2022; Received in revised form 14 November 2022; Accepted 22 November 2022

Available online 23 November 2022

0269-7491/© 2022 The Authors. Published by Elsevier Ltd. This is an open access article under the CC BY-NC-ND license (<http://creativecommons.org/licenses/by-nc-nd/4.0/>).

2015; Medina-Ramon et al., 2006). However, studies on the characteristics and disease-causing mechanisms of bacteria present in PM are limited, urging the need for further studies. *Pseudomonas stutzeri* (*P. stutzeri*; PS) is a non-fluorescent denitrifying bacterium present in soil and water, and is accountable for opportunistic infections in humans (Lalucat et al., 2006), causing wound and postoperative infections, as well as post-dialysis peritonitis (Goetz et al., 1983; Kalra et al., 2015; Noble and Overman, 1994). However, studies on the characteristics and pathogenicity of *P. stutzeri* PM101005 (PMPS) isolated from PM<sub>10</sub> are limited.

Toll-like receptors (TLRs) are key innate immune sensors that recognize microbial pathogen-associated molecular patterns and endogenous “risk” molecules released by host cells during infection, inflammation, or cellular stress (Kawasaki and Kawai, 2014). Till date, 13 mammalian TLRs have been identified, which have similar structural organization, consisting of a leucine-rich repeat-containing ectodomain involved in ligand recognition in their cytoplasmic tails, a transmembrane domain, and a TLR signaling domain (Jezierska et al., 2011). TLRs can be further classified by their ligands including lipids, proteins, or bacterial or viral nucleic acids. Some TLRs, such as TLR2–5, are present on the cell surface, whereas TLR3 and TLR7–9, are present on intracellular endosomes (Saitoh and Miyake, 2009). Signaling mechanisms of activated TLRs are critical for the control of bacterial infection via inflammation, but excessive inflammatory responses may lead to tissue damage (Dajon et al., 2017) and other side effects (Faure et al., 2000; Johnson et al., 2004). Thus, the classification of the activated TLRs and precise evaluation of their signaling mechanisms are important in controlling cellular damage.

Ambient air particles have been shown to induce cellular responses through specific TLRs (Arooj et al., 2020; Ryu et al., 2019; Woodward et al., 2017). Particularly, PM binding has been shown to activate TLR2 and TLR4, causing tissue damage by the secreted inflammatory cytokines. These inflammatory responses are regulated by polymyxin B treatment, indicating that these responses may be induced by bacteria present in PM (Shoenfelt et al., 2009). PM affects the host's response to infection, increasing the susceptibility to pathogenic bacteria. For instance, invasive infection of Group A *Streptococcus* (GAS) is increased by PM as they suppress macrophage phagocytosis and cytokine production through TLR/MAPK signaling (Zhi et al., 2022). Also, PM has been shown to promote infection by pathogenic bacteria, such as *Pseudomonas aeruginosa* PAO1, through mechanisms involving oxidative stress (Borcherding et al., 2013; Liu et al., 2019). These reports suggest that PM has the potential to increase the risk of bacterial infection after inhalation; therefore, the characterization and control of bacteria present in PM are essential for host defense.

Here, we examined the effect of inhaling PMPS on lung epithelial cells, alveolar cells, and macrophages, and elucidated the mechanisms through which PMPS induce inflammatory responses using both *in vitro* and *in vivo* experiments. Additionally, the types of antimicrobial peptides (AMPs) induced by the infection were identified, and their antibacterial effects on PMPS were assessed. The findings of this study would improve the understanding of the mechanism of PMPS in respiratory diseases.

## 2. Materials and Methods

### 2.1. Mice

TLR2, 4, and 5-deficient mice with C57BL/6 background were purchased from The Jackson Laboratory (Bar Harbor, ME, USA), and wild-type (WT) C57BL/6 mice were purchased from Koatech (Pyeongtaek, Korea). All animal studies were approved by the Institutional Animal Care and Use Committee of the Korea Research Institute of Bioscience and Biotechnology (Daejeon, Korea) (Approval No. KRIBB-ACE-21193).

### 2.2. Particulate matter

Fine dust ERM®-CZ100 (PM<sub>10</sub>) in amber glass vials was purchased from Sigma-Aldrich, Inc. (St. Louis, MO, USA) (Piaścik et al., 2019). PM<sub>10</sub> was suspended in phosphate-buffered saline (PBS), and immediately used in the experiments. The concentration of PM was adjusted based on previous studies to 1–100 µg/mL for *in vitro* experiments (Li et al., 2003; Yang et al., 2020) and to 200 µg/mice for *in vivo* (Budinger et al., 2011).

### 2.3. Preparation of bacteria

PMPS isolated from ERM®-CZ100 (GenBank: CP046902.1) and PS (ATCC 17588) were used in this study. Individual colonies of these bacteria cultured on Luria-Bertani (LB) plates were inoculated into 5 mL of LB broth and grown overnight at 37 °C under constant shaking (200 rpm). Subsequently, 1:5 dilution of the culture suspension was transferred to fresh medium and cultured for additional 2 h at 37 °C under constant shaking. The cells were collected by centrifugation at 10,000 g for 20 min, washed with PBS, pH 7.4, and re-suspended in sterile PBS to a concentration of 10<sup>9</sup> colony-forming units (CFU)/mL. The absorbance of bacterial suspensions was measured at 600 nm using a SpectraMAX 190 Microplate Reader (Molecular Devices, Menlo Park, CA, USA), and bacteria were diluted to the desired concentrations for use in each experiment.

### 2.4. Antibacterial activity assay

PMPS was cultured as described above, and 1 × 10<sup>5</sup> CFU of bacteria were incubated for 12 h with various concentrations of recombinant mouse β-defensin 3 (MRIHYLLFAFLLVLLSPPAAFSKKINNPVSLRKG GRCWNRCIGNTRQIGSCGVPFLKCCCKRK) (R&D Systems, Minneapolis, MN, USA) at 37 °C under constant shaking. The culture solution was subsequently plated onto LB agar to determine the number of living bacteria.

### 2.5. Cell culture and bacterial infection

Bone marrow-derived macrophages (BMDMs) were prepared as previously described (Celada et al., 1984). MH-S cells were grown in RPMI 1640 medium (Corning, Thermo Fisher Scientific, Waltham, MA, USA) containing 10% FBS (HyClone, Logan, UT, USA) and supplemented with 5.0 µg/mL of streptomycin and 5.0 U/mL of penicillin. MLE-12 cells were maintained in DMEM/F12 (Corning, Thermo Fisher Scientific) containing 2% FBS supplemented with 5.0 µg/mL of streptomycin and 5.0 U/mL of penicillin. 16HBE14o-cells were maintained in MEM (Corning, Thermo Fisher Scientific) supplemented with 2 mM of L-glutamine (Corning, Thermo Fisher Scientific), 10% FBS, 1% (5.0 µg/mL) streptomycin, and 5.0 U/mL of penicillin. BMDMs were seeded into 12-well plates at a concentration of 1 × 10<sup>6</sup> cells/well and incubated overnight at 37 °C in a 5% CO<sub>2</sub> incubator. MLE-12 and MH-S cells were seeded in 12-well plates at a concentration of 2 × 10<sup>5</sup> cells/well and infected with PS or PMPS at indicated multiplicity of infection (MOI) for 60 min, with extracellular bacterial growth inhibited by treatment with gentamicin (50 µg/mL). Culture supernatants and cell lysates were collected at the indicated post-infection time points for further analysis.

### 2.6. 3D spheroid cultures

3D human pulmonary alveolar epithelial cell spheroids kit (SP3D-3210) was purchased from ScienCell Research Laboratories (Carlsbad, CA, USA) and cultured according to the manufacturer's instructions. Briefly, each frozen vial containing ≥4.0 × 10<sup>3</sup> spheroids was thawed and re-suspended in 3D Epithelial Spheroid Medium containing 2% FBS, or in 3D Kidney Spheroid Medium containing 5% FBS; each of these

media was supplemented with the reagents included in the kit. After resuspension, approximately 167 spheroids were seeded in a 24-well Ultra-Low Binding Culture Plate (provided in the kit) and incubated at 37 °C for 24 h, followed by the replacement of 70% of the culture medium with fresh medium and further incubation for 3 d. Thereafter, 70% of the culture medium was replaced with fresh medium, followed by further incubation for 24 h.

## 2.7. Infectivity analysis

BMDMs ( $2 \times 10^5$  cells/well) and MLE-12 and MH-S cells ( $5 \times 10^4$  cells/well) were seeded in 48-well plates and incubated overnight at 37 °C in a 5% CO<sub>2</sub> incubator, followed by infection with PS and PMPS at a MOI of 1/10. At the indicated time points, the cells were washed three times with cold PBS and lysed with 1% Triton X-100 in PBS. Cell lysates were plated in LB agar to determine the number of living bacteria in the lysates. PS and PMPS were labeled with BacLight Red (Molecular Probes, Eugene, OR, USA), according to the manufacturer's instructions. MLE-12, MH-S, and BMDMs were infected with labeled bacteria as described above. After 1 h, the cells were fixed in 4% paraformaldehyde for 15 min at room temperature (20–22 °C), and then washed with ice-cold PBS. Nuclei were counterstained with 4',6-diamidino-2-phenylindole dihydrochloride (DAPI, Invitrogen, Carlsbad, CA, USA), and cellular uptake of bacteria was measured using an EVOS M5000 fluorescence microscope (Invitrogen).

## 2.8. Cell viability

Cell viability was determined using WST assay (Dogen, Seoul, Korea). Briefly, BMDMs ( $2.5 \times 10^5$  cells/well) and MLE-12 and MH-S cells ( $2.5 \times 10^4$  cells/well) were seeded in 96-well plates and incubated overnight at 37 °C, followed by infection with PS and PMPS at indicated MOI and further incubation for 24 h. Thereafter, WST solution was added (10 µL of WST solution per 100 µL of cell culture medium) and the plates were incubated for 2 h, and absorbance was measured at 450 nm using a microtiter plate reader (Molecular Devices, San Jose, CA, USA).

## 2.9. Caspase-3/7 activity

BMDMs ( $1 \times 10^6$  cells/well), and MLE-12 and MH-S cells ( $1 \times 10^5$  cells/well) were seeded in 12-well plates and cultured overnight at 37 °C, followed by infection with PS and PMPS at indicated MOIs for 24 h. After incubation, the cells were washed three times with PBS and lysed with lysis buffer containing protease inhibitors. Caspase-3/7 activity was measured using Caspase-Glo 3/7 Assay Kits (Promega Corp., Madison, WI, USA), according to the manufacturer's instructions.

## 2.10. Determination of *in vivo* virulence

TLR2, 4, and 5-deficient mice and WT mice aged 8–9 weeks were used in all infection experiments. Bacteria were cultured as described above. For infection of mice, PS and PMPS were washed in sterile PBS and diluted to the appropriate density, and each mouse was intranasally (i.n.) inoculated with  $3 \times 10^8$  CFU of the bacteria. Blood samples were collected with heparinized capillary tubes (Scientific Glass Inc., USA) by orbital venous plexus bleeding. Serum was isolated by centrifugation at 3000 rpm for 20 min and stored in a freezer at –80 °C for further analysis. PS and PMPS-infected mice were sacrificed at the indicated times and their lungs were collected. To determine bacterial growth, each homogenate was incubated on LB agar plates for 2 d at 37 °C in an incubator, the numbers of colonies were counted, and the number of bacteria was calculated (measured as CFU/g tissue).

## 2.11. Histopathological examination

The right lobes of the lungs were weighed and homogenized in PBS, and half of each lysate was diluted with sterile PBS, plated in LB agar plates, and incubated at 37 °C for 1–2 d. The colonies were counted and the number of bacteria was calculated (measured as CFU/g lung tissue). The other half of each lysate was centrifuged and the supernatant was stored at –80 °C in a freezer for cytokine measurement. Lungs were harvested and fixed in 10% neutral formalin for histopathological analysis. The tissues were processed through an alcohol and xylene series and then embedded in paraffin. Subsequently, 4 µm-thick sections were prepared, stained with hematoxylin and eosin (H&E), and examined using a microscope (EVOS M5000, Thermo Fisher Scientific). Lung sections from each group (n = 15–20 areas per section) were scored for edema, neutrophil margination and tissue infiltration, intra-alveolar hemorrhage, debris, and cellular hyperplasia. Each histological site was assigned a value of 1 (normal), 2 (minimum), 3 (mild), 4 (moderate), or 5 (severe), and the average score for each group was calculated. All slides were presented in random order and analyzed in a blinded manner.

## 2.12. Cytokine measurement

The concentrations of mouse IL-1β, IL-6, IL-10, MCP-1, MIP-1α, and tumor necrosis factor-α (TNF-α), and human IL-6, IL-8, and IL-1β (Thermo Fisher Scientific, Waltham, MA, USA), and mouse CXCL1 (R&D Systems) in culture supernatants of PS and PMPS-infected BMDMs and MLE-12 and MH-S cells, and in tissue lysates from infected mice, were determined using ELISA kits, according to the manufacturer's instructions.

## 2.13. Albumin concentration in bronchoalveolar lavage fluid (BALF)

After euthanasia, BALF was collected by catheterizing the trachea and washing the lungs twice with 1 ml of ice-cold PBS containing a protease inhibitor (Merck, Merck, Kenilworth, NJ, USA). Cells were removed by centrifugation (4000 rpm, 5 min, 4 °C) and BALF was obtained and stored at –80 °C. Albumin concentrations were determined in BALF using the BCG Albumin Assay Kit (Sigma-Aldrich) according to the manufacturer's protocol.

## 2.14. Immunoblotting

Protein was extracted from whole cell extracts using CETi lysis buffer (TransLAB, Daejeon, Korea) supplemented with protease inhibitor (GenDEPOT, Barker, TX, USA) and phosphatase inhibitor (GenDEPOT). The cells were washed once with DPBS, suspended in 200 µL of CETi buffer, and collected by scraping. Total protein was separated from cell debris by centrifugation at 13,000 rpm for 5 min and quantified using Pierce® BCA Protein Assay Kit (Thermo Fisher Scientific). The proteins were loaded onto Bolt™ 4–12% Bis-Tris Plus Gels (Invitrogen), electrophoresed, and transferred onto polyvinylidene difluoride (PVDF) membranes. The membranes were blocked by incubating in PVDF blocking reagent (Toyobo Co., Ltd., Osaka, Japan) for 1 h, washed three times for 5 min each with TBST (20 mM Tris [pH 7.6], 137 mM NaCl, 0.1% Tween 20), and incubated with primary antibodies overnight at 4 °C. The primary antibodies include rabbit anti-NF-κB p65, rabbit anti-phospho-NF-κB p65 (Ser536), rabbit anti-phospho-p44/42 MAPK (ERK1/2) (Thr202/Tyr204), rabbit anti-phospho-SAPK/JNK (Thr183/Tyr185), rabbit anti-phospho-p38 MAPK (Tr180/Tyr182), and horseradish peroxidase (HRP)-conjugated anti-rabbit β-actin (Cell signaling Technology, Beverly, MA, USA). Thereafter, the membranes were washed three times and incubated in the dark with secondary antibodies labeled with horseradish peroxidase for 1.5 h at room temperature. Images were detected using the Western Lightning Chemiluminescence System (Atto Co., Tokyo, Japan).

### 2.15. Transcriptome analysis

Total RNA was extracted using NucleoSpin RNA Plus columns (Macherey-Nagel, Dürren, Germany), reverse transcribed to cDNA using reverse transcriptase, and amplified using NanoHelix RT-qPCR kits (NanoHelix, Daejeon, Korea). The PCR cycling conditions were as follows: an initial cycle at 50 °C for 2 min and denaturation at 95 °C for 10 min to activate the DNA polymerase, followed by 40 cycles of denaturation at 95 °C for 15 s, annealing at 60 °C for 30 s, and final extension at 72 °C for 30 s. SYBR Green technology was used to quantify the results. Data were analyzed using LightCycler® 96 System Analysis Software (Roche Diagnostics GmbH, Mannheim, Germany). The relative expression of each gene was normalized to the expression of GAPDH in the same sample. The primers used for real-time PCR are shown in Table 1.

### 2.16. Transmission electron microscopy (TEM)

PS and PMPS were cultured at 37 °C with shaking for 2 h, centrifuged at 3000 rpm for 20 min to obtain a cell pellet, and then diluted with 1 ml of PBS. A drop of bacterial solution was placed on a copper grid and air dried for 5 min. Bacterial morphology was investigated using an energy-filtered transmission electron microscope (Libra 120, Carl Zeiss, Oberkochen, Germany) operating at an accelerating voltage of 120 kV after staining with 2% phosphotungstic acid (PTA).

### 2.17. Phylogenetic analysis and genome sequencing

For identification of PS and PMPS, 16S ribosomal RNA (rRNA) gene-based PCR and sequencing were performed. Primers of 27F (5'-AGAGTTTGATCMTGGCTCAG-3') and 1492R (5'-TACGGY-TACCTTGTACGACTT-3') were used for 16S rRNA gene amplification. 16S rRNA gene amplification sequencing was performed at Solgent (Solgent Co, Daejeon, Korea) using Big Dye Terminator Cycle Sequencing Kit and ABI PRISM 3730 DNA Analyzer (PE Applied Biosystem, Foster, CA, USA). Sequence similarity was further analyzed using BLAST from the National Center of Biotechnology Information (NCBI) website. The phylogenetic tree was constructed using the neighbor joining method using MEGA7 software (Kumar et al., 2016).

### 2.18. Biological characterization

Biochemical characterization of PS and PMPS was performed using commercial API 20NE and API ZYM kits according to the manufacturer's instructions (bioMérieux, Marcy l'Etoile, France). Cell growth of PS and PMPS was monitored at 4, 10, 18, 25, 30, 37, 42 and 45 °C, respectively. Growth at various initial pH values (pH 3–11 with 0.5 pH unit intervals)

was evaluated after incubation for 7 days at 30 °C using marine broth. The pH of the marine broth was adjusted using the following buffers (20 mM each final concentration): acetate buffer for pH 4.0–5.5, phosphate buffer for pH 6.0–8.0 and Tris buffer for pH 8.5–10.0. Salt tolerance was tested in marine broths, where the concentration of sodium chloride was adjusted from 0.5 to 10.0% NaCl and growth was assessed after incubation at 30 °C for 7 days.

### 2.19. Statistical analysis

Statistical significance between groups was determined by a two-tailed Student's t-test or one-way analysis of variance followed by post-hoc analysis (Bonferroni's multiple comparisons test and Tukey's post-hoc test). Means were considered significant at  $p < 0.05$ , and all statistical analysis were performed using GraphPad Prism 5 (GraphPad Software, La Jolla, CA).

## 3. Results

### 3.1. PS and PMPS induced inflammatory responses in BMDMs, and in MLE-12 and MH-S cells

We first present the results of analyzing the TEM image, phylogenetic tree, API test, temperature, pH, and growth conditions by NaCl concentration, which were performed to investigate the characteristics of PS and PMPS (Supplementary Fig. 1). Various studies related to lung damage from PM inhalation have been performed using lung epithelial cells and alveolar macrophages (Guohua et al., 2021; Neri et al., 2016). The ability of PM-derived PMPS to induce inflammatory responses in the lung epithelial cell line MLE-12, the lung alveolar macrophage cell line MH-S, and BMDMs was evaluated. Infection with PS and PMPS increased the secretion of inflammatory cytokines and chemokines by the cells, with BMDMs exhibiting a higher production of the cytokines and chemokines. Particularly, infection with PS and PMPS significantly increased the secretion of the chemokines in MLE-12 cells, and the secretion of IL-6, IL-1 $\beta$ , and MCP-1 in MH-S cells; however, PMPS-treated cells had generally higher levels of the cytokines and chemokines than PS-treated cells (Fig. 1A). Additionally, the NF- $\kappa$ B and MAPK activities of the infected cells were evaluated, as both NF- $\kappa$ B and MAPK are involved in the induction of inflammatory cytokines and chemokines. Infection with PS and PMPS induced the phosphorylation of p38, JNK, ERK, and p65 in BMDMs within 60 min, and phosphorylation of the sites in MLE-12 and MH-S cells with 15 min; however, PMPS had a greater effect than PS on the pathways in BMDMs (Fig. 1B). Furthermore, we examined the effect of PS and PMPS on the mRNA and protein expression of IL-6 and IL-8 in the human bronchial epithelial cell line 16HBE14o-, after 6 and 18 h of infection. Infection with PS and

**Table 1**  
Primers used for qPCR.

Gene	Primers (5'-3')	
	Forward	Reverse
mCp-2	ACTGAGGAGCAGTCAGGTGAA	GCCAATGGTCATCTTGTCTCT
mCp-3	CAGGCTGTGTCTGTCTCTTTTG	TCAGCGACAGCAGAGTGTGTA
mCp-4	CAGGTCCAGGCTGATCCTATC	AAGTCCACGAACCTCGTCTCTC
mCp-5	TGTCTCTCTCTCTGCGCTTGT	ATGAAGAGCAGACCCCTTCTTGG
mBD-1	CACATCTCTCTGCACTCTGGAC	CCATCGCTCGTCTTTATGCCATTG
mBD-2	GCCATGAGGACTCTCTGCTC	AGGGGTCTCTCTCTGGGAAA
mBD-3	TCTGTTTGCAATTTCTCTGGTG	TAACTTCCAACAGCTGGAGTGG
mBD-4	TCTGTTTGCAATTTCTCTGGTG	TTTGCTAAAAGCTGCAGGTGG
mBD-6	TCATGAAGATCCATTACCTG	TGTGCATATTACGAAGAAG
mCRAMP	CTCGAGATGCAGTCCAGAG	GCGGCCGAGAGACCCTACT
mGAPDH	GTGGAGATTGTGCCATCAACG	CAGTGGATGCAGGGATGATGTTCTG
hIL-6	TTCTCCACAAGCGCCTTC	GGAATCTTCTCTCTGGGGTA
hIL-8	AGCTGATGGCCCTAAACAGA	CATCCAGAGGCGAGAGTTC
hIL-1 $\beta$	GCTGAGGAAGATGCTGGTTG	GAAGGGAAGAAGGTGCTCA
hGAPDH	GCACCGTCAAGGCTGAGAAC	TGGTGAAGACGCCAGTGA



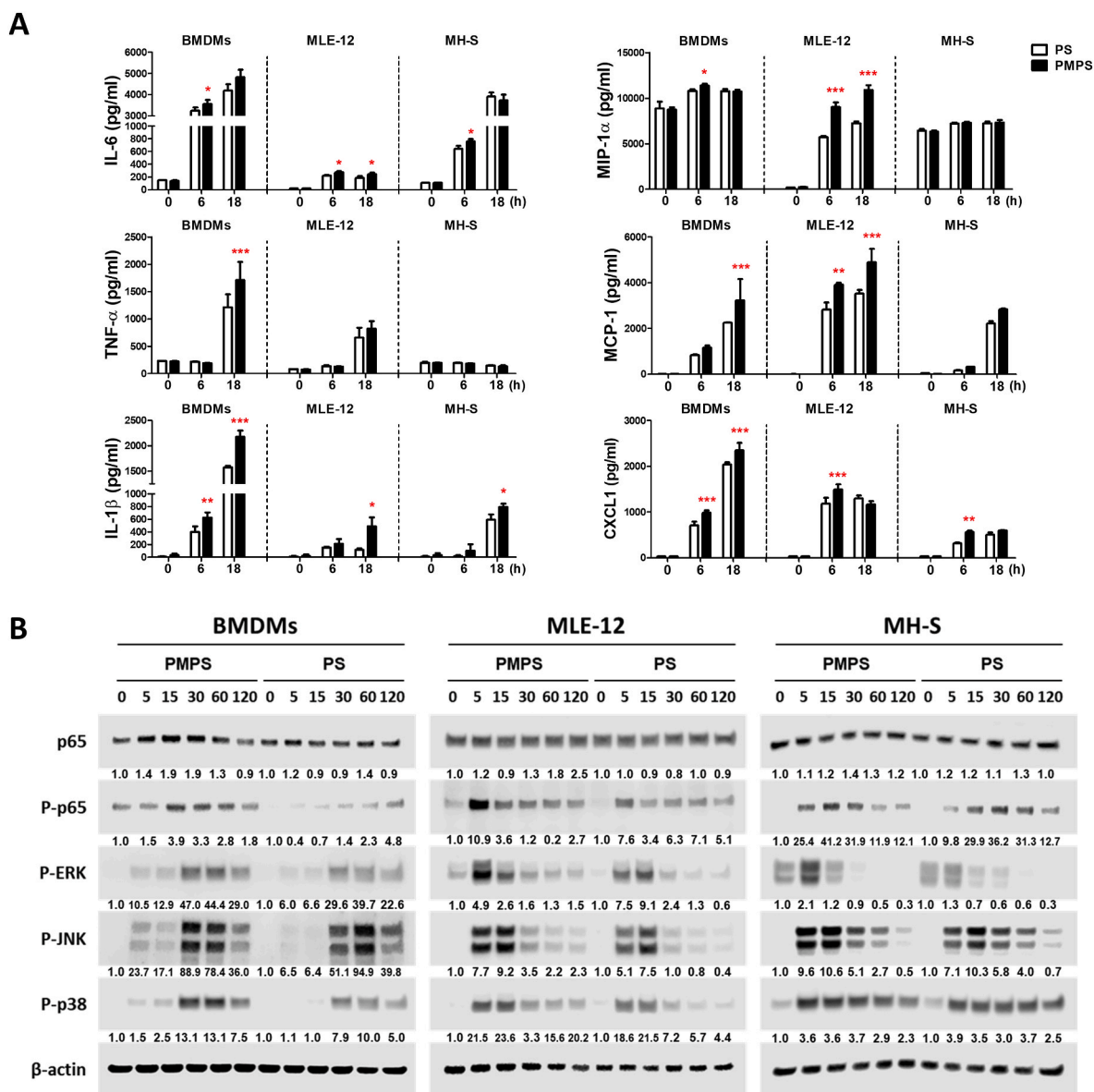


**Fig. 1.** PS and PMPS induce inflammatory responses in BMDMs, and in MLE-12 and MH-S cells. **A.** BMDMs, and MLE-12 and MH-S cells were infected with PS and PMPS at MOIs of 1/10 and treated with gentamicin 1 h later. The concentrations of IL-6, TNF- $\alpha$ , IL-1 $\beta$ , CXCL1, MCP-1, and MIP-1 $\alpha$  in the culture supernatants were determined by ELISA at 6 and 18 h after infection, and the results were expressed as the mean  $\pm$  standard deviation (SD) of three independent experiments. **B.** BMDMs (MOI 1/10), and MLE-12 and MH-S cells (MOI 1/50) were infected with PS and PMPS and then treated with gentamicin 1 h later. Cell lysates were collected at the indicated time points and analyzed by Western blotting. Equal loading was confirmed by Western blotting using antibodies against  $\beta$ -actin. The results are representative of two independent experiments. The quantification was performed by dividing the densities of each molecule by that of  $\beta$ -actin. Values are shown below the corresponding figures. \* $p < 0.05$ , \*\* $p < 0.01$ , and \*\*\* $p < 0.001$ .

PMPS increased the expression of IL-6 and IL-8 in 16HBE14o- at both the mRNA and protein levels (Supplementary Fig. 2). Overall, these results indicated that PMPS infection activated signaling pathways involved in inflammatory cytokine and chemokine production.

### 3.2. Infectivity and cytotoxicity of PS and PMPS in BMDMs, and MLE-12 and MH-S cells

Since bacterial infectivity is an important consideration regarding its pathogenicity, the infectivity of PS and PMPS was evaluated in BMDMs, MH-S, and MLE-12 cells. There was an intracellular increase in the population of both PS and PMPS in a time-dependent manner for up to 2 h after infection, with the number of PMPS higher than that of PS (Fig. 2A). Consistently, PMPS showed higher infectivity when the cells were infected with fluorescently-labeled bacteria (Fig. 2B), indicating

that PMPS was more infective than PS in lung epithelial cells, lung alveolar macrophages, and macrophages. Since the high infectivity of the bacteria leads to excessive inflammatory responses and cytotoxicity, we then examined the viability of these infected cells. There was a dose-dependent decrease in the viability of the cells with increasing bacterial concentration 24 h after infection. Particularly, the viabilities of BMDMs and MLE-12 cells decreased to less than 50% following bacterial infection at MOIs of 1/10 and 1/50, respectively (Fig. 2C). Moreover, there was an increase in caspase-3/7 activity with increasing bacteria concentration, confirming bacteria-induced cell apoptosis. Intriguingly, PMPS-infected cells had higher caspase-3/7 activity than PS-infected cells (Fig. 2C). These results indicated that PMPS promoted the death of lung epithelial cells, lung alveolar macrophages, and macrophages at a greater extent than PS infection.

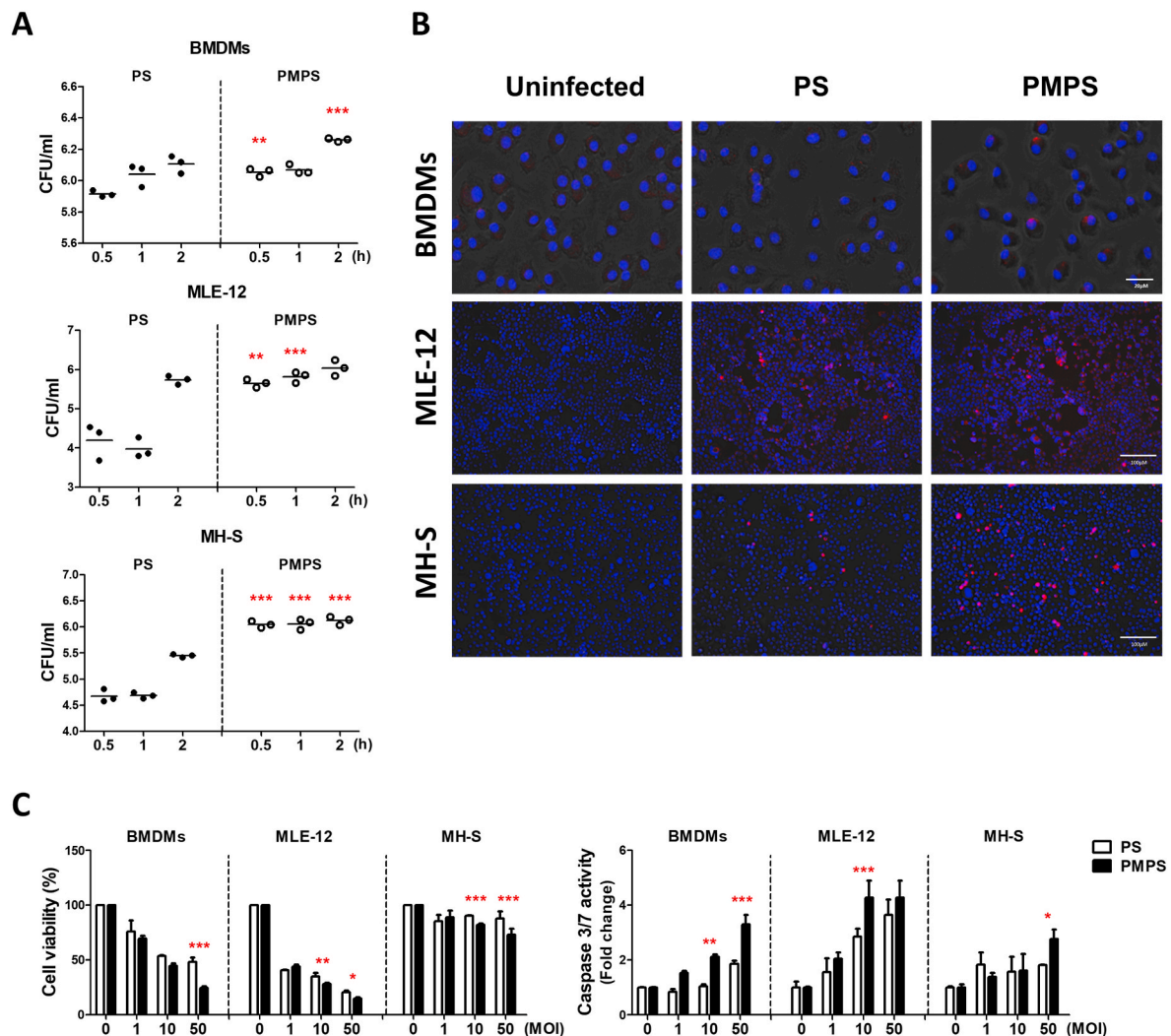


**Fig. 2.** Infectivity and cytotoxicity of PS and PMPS in BMDMs, and in MLE-12 and MH-S cells. **A.** BMDMs, and MLE-12 and MH-S cells were infected with PS and PMPS at indicated MOI. After incubation for 0.5, 1, and 2 h, cell lysates were plated on LB agar and incubated overnight. The results are expressed as the mean  $\pm$  SD of three independent experiments. **B.** Cells were infected with BacLight Red-labeled PS and PMPS at an MOI of 1/10. After 2 h, the cells were washed three times with PBS and analyzed using a flow cytometer and confocal microscope to quantify intracellular BacLight Red-labeled bacteria. Cell nuclei were counter stained with DAPI (blue). Scale bar: BMDMs, 20  $\mu$ m; MLE-12 and MH-S, 100  $\mu$ m. **C.** The cells were infected with PS and PMPS at the indicated MOIs and treated with gentamicin for 90 min after infection, and cell viability was determined 24 h after infection using WST and Caspase-3/7 activity assays. Cell viability (%) and Caspase-3/7 activity were expressed as a comparison with those of uninfected (MOI, 0) control cells. The results are representative of three independent experiments. \* $p < 0.05$ , \*\* $p < 0.01$ , and \*\*\* $p < 0.001$ . (For interpretation of the references to colour in this figure legend, the reader is referred to the Web version of this article.)

### 3.3. Analysis of inflammatory responses induced by PS and PMPS in human airway spheroids

For decades, conventional 2D cell culture have been used to study the pathology of various cell types; however, these systems may not fully recapitulate the complex physiological environment of bronchial epithelial cells. This gave rise to the 3D cell culture methods which allow reproduction of the human bronchial epithelium more precisely. Here, the effect of PMPS and PS on cytokine production by human airway spheroids was examined. Consistent with results obtained in lung epithelial cells, lung alveolar macrophages, and macrophages, infection with both PS and PMPS significantly increased the secretion of inflammatory cytokines (IL-6, IL-8, and IL-1 $\beta$ ) by human airway spheroids, with PMPS having a greater effect on cytokine production than PS (Fig. 3). Overall, these results suggested that PMPS infection induced higher inflammatory responses in human airway spheroids than from PS infection.

### 3.4. Pathogenicity of PS and PMPS in mice

Furthermore, we evaluated whether the *in vitro* infectivity of PMPS in lung epithelial cells, alveolar macrophages, and macrophages was reproduced in animal models. Experimental mice were infected with PS and PMPS, and we enumerated the bacteria in the lungs. The lungs of PMPS-infected mice had significantly higher bacterial count (CFU) than those of PS-infected mice (Fig. 4A). Additionally, histological analysis showed that lung tissue damage was more severe in PMPS-infected mice than in PS-infected mice (Fig. 4B). Moreover, serum concentrations of IL-6, TNF- $\alpha$ , MCP-1, and MIP-1 $\alpha$  were higher in PMPS-infected mice than in PS-infected mice. The TNF- $\alpha$  concentration of the lungs of PMPS-infected mice was remarkably higher than those of PS-infected mice; however, the concentrations of the other cytokines and chemokines were comparable between the two groups (Fig. 4C). Overall, these results indicated that PMPS, which showed greater infectivity, induced higher inflammatory responses than PS in mice.

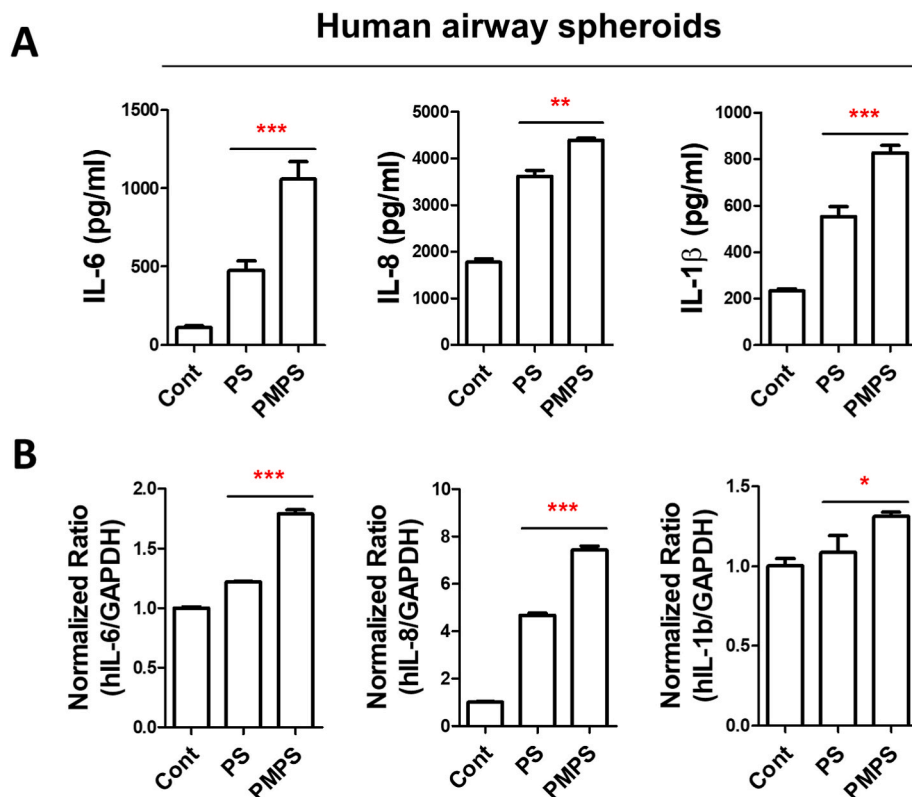


**Fig. 3.** PS and PMPS induce inflammatory responses in human airway spheroids. A. Human airway spheroids were infected (or not) with bacteria for 24 h and then the supernatant was collected. The IL-1 $\beta$ , IL-6, and IL-8 levels of the supernatants were assessed using a commercially available ELISA kit. B. Real-time qRT-PCR analysis of expression levels of the cytokine gene. Data were normalized to GAPDH (loading control) expression level. The results are representative of three independent experiments. \* $p < 0.05$ , \*\* $p < 0.01$ , and \*\*\* $p < 0.001$ .

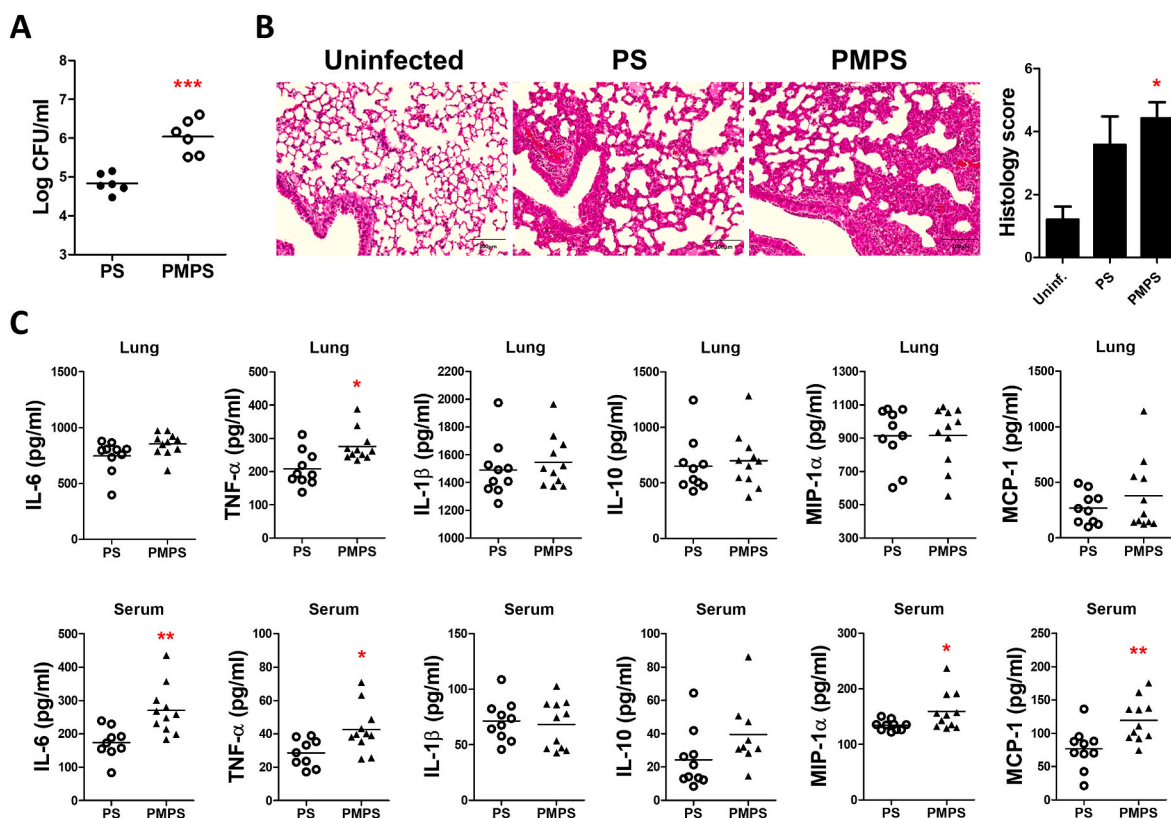


**Fig. 4.** Assessment of PS and PMPS pathogenicity in mice. A. Mice were inoculated intranasally with  $3 \times 10^7$  CFU of PS and PMPS. The bacterial loads of the lungs were evaluated 24 h later. PS group:  $n = 6$ , PMPS group:  $n = 6$ . B. Histologic examination of lung tissue samples stained with H&E, as described in the Materials and Methods section. Scale bar: 100  $\mu$ m. Histology scores are expressed as the mean  $\pm$  SD of 5–7 mice per group. C. Serum and lung tissue samples were collected 24 h after infection, and the concentrations of cytokines and chemokines were measured using commercially available ELISA kits. Each dot represents an individual mouse. PS group:  $n = 10$ , PMPS group:  $n = 11$ . \* $p < 0.05$  and \*\* $p < 0.01$ .



### 3.5. PM treatment exacerbated PMPS-induced inflammatory responses and pathogenicity

PM exposure has been reported to induce oxidative stress and impair tight junctions, thereby promoting bacterial infection and/or inhibiting antimicrobial activity (Chen et al., 2018). Therefore, we examined the effect of PM treatment on PMPS-induced inflammatory response, infectivity, and cell death in BMDMs. PM treatment enhanced the production of IL-6, IL-1 $\beta$ , and MCP-1 by PMPS-infected BMDMs in a dose-dependent manner (Fig. 5A). Moreover, PM treatment increased PMPS infection rate and enhanced PMPS-induced decrease in cell viability (Fig. 5B and C). Similar results were obtained from mice, as indicated by the bacterial loads of the lungs and histological analysis (Fig. 5D and E). Furthermore, the albumin levels of BALF from PMPS- and PM-treated mice were measured as an indicator of lung injury, due to the association of elevated pulmonary albumin levels with lung epithelial leakage caused by lung injury (Eckle et al., 2013; Meissner et al., 2005). Although PMPS infection itself increased the albumin levels of BALF from the mice, PM treatment further enhanced PMPS-induced increase in the albumin level (Supplementary Fig. 3) suggesting that fine dust exacerbates PMPS-induced increase in inflammatory responses and tissue damage.

### 3.6. TLRs mediated PMPS-induced inflammatory responses

So far, studies are yet to elucidate the immune receptors through which PMPS induce inflammatory responses after infection. In the present study, infection of PMPS induced inflammatory cytokine production by BMDM and MLE-12 and MH-S cells through NF- $\kappa$ B and MAPK pathways (Fig. 1). As pattern-recognition-receptors, TLRs of macrophages and epithelial cells play an essential role in the clearance of bacteria through pathogen-associated molecular patterns (PAMP) recognition (Dajon et al., 2017). TLR2, TLR4, and TLR5 activate NF- $\kappa$ B and MAPK signaling through the bacterial cell wall or flagella recognition and induce the production of various inflammatory cytokines. To investigate whether TLRs are accountable for the inflammatory responses following PMPS infection, we infected TLR2-, TLR4-, and TLR5-deficient BMDMs with PMPS. Following PMPS infection, the production of evaluated cytokines and chemokines was largely reduced in TLR4-deficient BMDMs, and the production of IL-1 $\beta$ , IL-10, and MCP-1 was also reduced in TLR2-deficient BMDMs compared with WT cells (Fig. 6A). Similarly, phosphorylation of p65, JNK, ERK, and p38 was reduced in PMPS-infected TLR2- and TLR4-deficient cells relative to WT cells (Fig. 6B and Supplementary Fig. 4). Overall, these results demonstrated that PMPS-induced inflammatory responses in BMDMs were mediated by TLR2 and TLR4 signaling mechanisms.

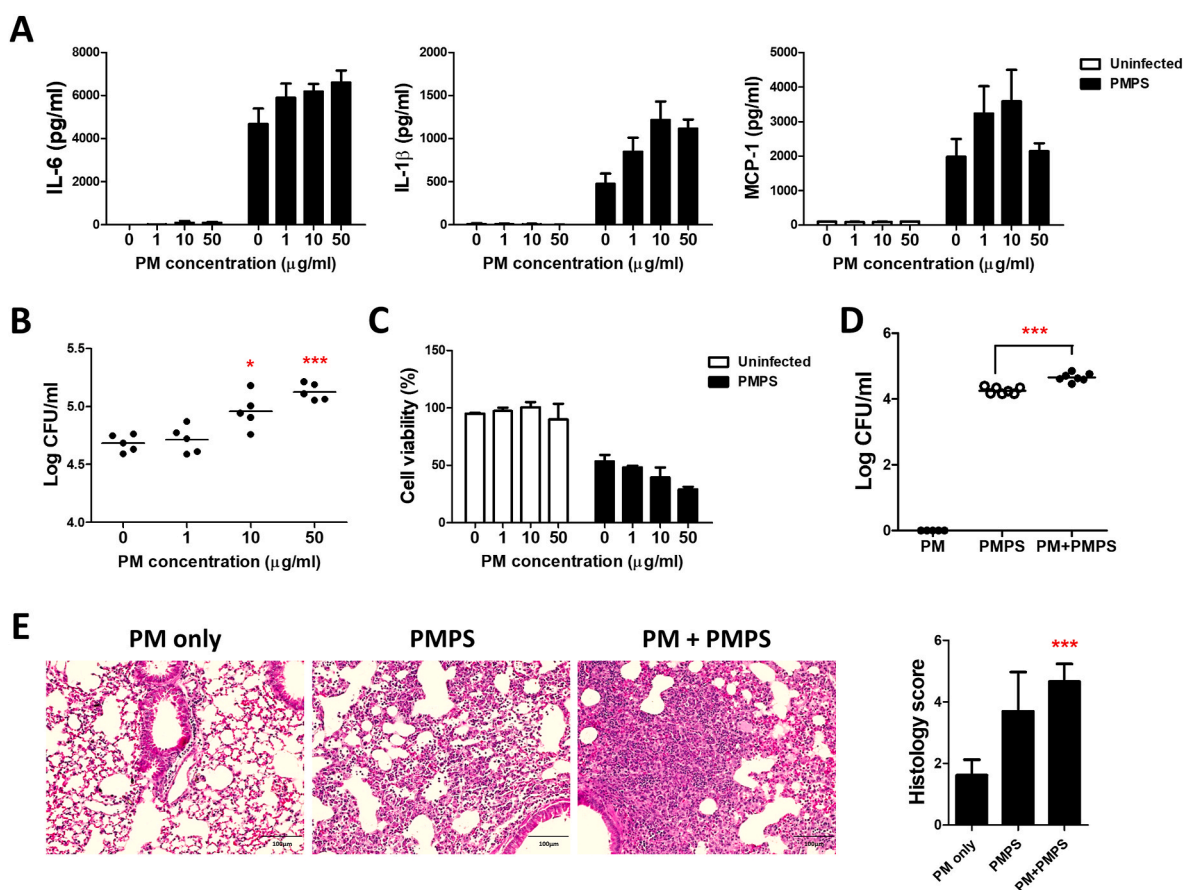


**Fig. 5.** Effect of PM treatment on PMPS infection-induced pathogenicity. A and B. BMDMs were treated with various doses (1, 10, 50  $\mu$ g/ml) of PM 24 h prior to infection, followed by infection with PMPS at an MOI of 1/10 and treatment with gentamicin 1 h later. The concentrations of IL-6, IL-1 $\beta$ , and MCP-1 in the culture supernatants were measured 18 h post-infection using ELISA kits, and cell viability was determined using WST assays. Data were expressed as % viability compared with the uninfected control. C. BMDMs treated with indicated concentrations of PM for 24 h were infected with PMPS for 1 h. Cell lysates were plated on LB agar and incubated overnight. Data were expressed as the mean  $\pm$  SD of three independent experiments. The results were based on data obtained from one of two independent experiments. D and E. Mice were inoculated intranasally with  $3 \times 10^8$  CFU of PMPS and 200  $\mu$ g of PM/mice, and their lungs were harvested 24 h after infection. The bacterial loads of the lungs were determined, and the sections were stained with H&E for histological assessment. Scale bar: 100  $\mu$ m. Histology scores were expressed as the mean  $\pm$  SD of 5–7 mice per group. PM only group: n = 5, PMPS group: n = 7, PM + PMPS group: n = 7. \*p < 0.05 and \*\*\*p < 0.001.

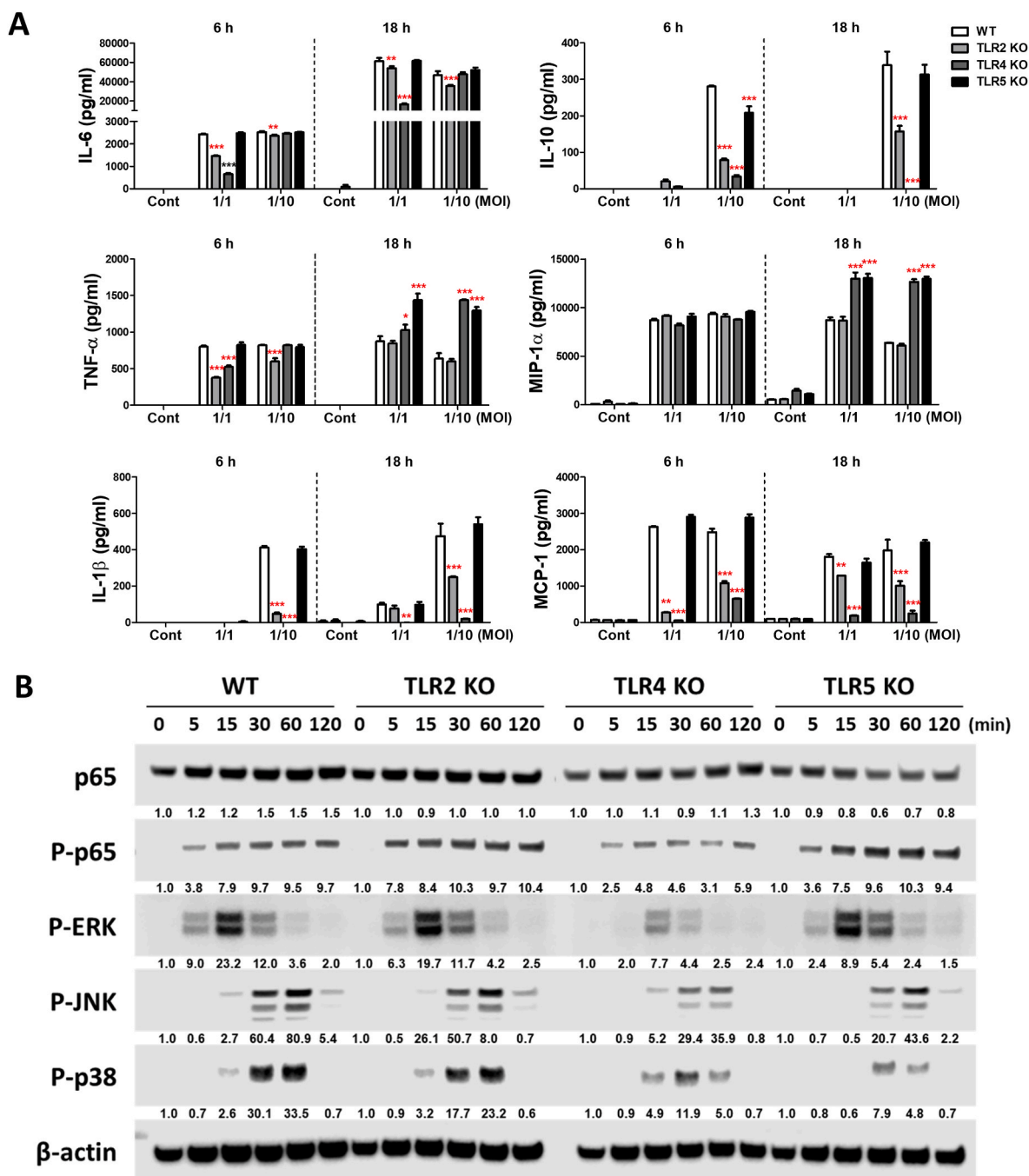


**Fig. 6.** PMPS induces TLR2-, TLR4-, and TLR5-dependent inflammation through NF- $\kappa$ B and MAPK signaling. **A.** WT and TLR2-, TLR4-, and TLR5-deficient BMDMs were infected with PMPS at MOIs of 1/1 and 1/10, and treated with gentamicin 1 h later. The concentrations of IL-6, TNF- $\alpha$ , IL-1 $\beta$ , IL-10, MCP-1, and MIP-1 $\alpha$  in the culture supernatants were determined 18 h after infection using an ELISA kit. **B.** Cell lysates were collected at the indicated time points and analyzed by Western blotting. Equal loading was confirmed by Western blotting of the same samples using antibodies against  $\beta$ -actin. The results shown are representative of one of two independent experiments. The quantification was performed by dividing the densities of each molecule by that of  $\beta$ -actin. Values are shown below the corresponding figures. \* $p < 0.05$ , \*\* $p < 0.01$ , and \*\*\* $p < 0.001$ .

### 3.7. TLR deficiency in mice increased the pathogenicity of PMPS

We further evaluated whether TLR-mediated inflammatory responses in PMPS-infected BMDMs show similar dependency *in vivo*. Relative to the observations with WT mice, CFUs of PMPS in the lungs were robustly increased in TLR2-, TLR4-, and TLR5-deficient mice 1 and 3 d post-infection (Fig. 7A). Additionally, PMPS-infected TLR2-, TLR4-, and TLR5-deficient mice showed higher levels of several cytokines and chemokines in the lungs and serum compared with those of WT mice (Fig. 7B). Histological analysis also showed an increase in cell

infiltration in TLR2-, TLR4-, and TLR5-deficient mice compared with WT mice (Fig. 7C). These results demonstrated the critical role of TLR2, TLR4, and TLR5 in bacterial control and inflammation in the lung of PMPS- infected mice.

### 3.8. Evaluation of types and antibacterial activity of AMPs induced by PMPS

AMPs, which are secreted by various cells in response to bacterial infection, play an important role in eliminating bacteria. We, therefore,



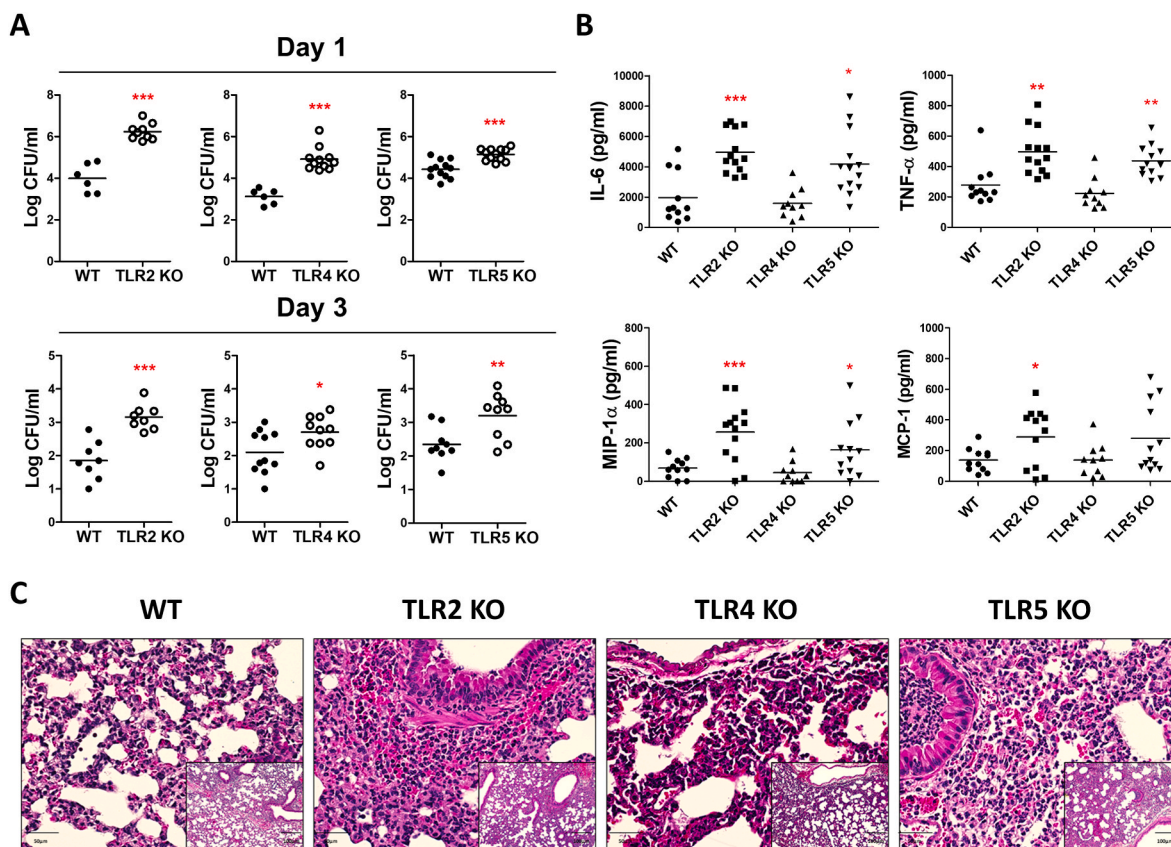


**Fig. 7.** PMPS infectivity and tissue damage in mice is dependent on TLR2, TLR4, and TLR5. **A.** TLR2, TLR4, and TLR5 KO mice were inoculated intranasally with  $3 \times 10^7$  CFU of PMPS, and the bacterial loads of the lungs were determined 1 and 3 d after infection. WT ( $n = 6$ ) vs TLR2 KO ( $n = 9$ ), **B.** The concentrations of IL-6, TNF- $\alpha$ , MCP-1, and MIP-1 $\alpha$  in serum samples collected from the mice 24 h post-infection were determined using commercially available ELISA kits. **C.** Histologic examination of lung tissue samples collected 24 h post-infection was performed as described in the Materials and Methods section. Each panel represents a cell displayed at a higher magnification than that shown in the inset. Scale bar: 50  $\mu$ m, inset: 100  $\mu$ m. Each dot represents an individual mouse. \* $p < 0.05$ , \*\* $p < 0.01$ , and \*\*\* $p < 0.001$ .

investigated the effect of PMPS infection on the expression of AMPs, such as  $\alpha$ - and  $\beta$ -defensin and cathelicidin. PMPS infection increased the expression of some AMPs in BMDMs, MLE-12, and MH-S cells, among which BD3 was the most expressed in MH-S cells and BMDMs in a TLR2- and TLR4-dependent manner (Fig. 8A and B). Additionally, recombinant BD3 showed an antibiotic effect against PMPS, with BD3 concentrations of 5–10  $\mu$ g/mL significantly reducing the number of PMPS (Fig. 8C). Yet, a previous study reported the reduction of *P. aeruginosa* PA01-induced h-BD2 in the presence of PM (Chen et al., 2018). Likewise, we observed that PM treatment reduced the PMPS-induced increase in BD3 expression (Fig. 8D). These observations show that BD3 expression mediated through TLR signaling after PMPS infection is crucial for bacterial control, but the presence of PM reduces BD3 production.

#### 4. Discussion

Inflammatory responses to fine dust have been found to cause airway inflammation (Li et al., 2002; Schaumann et al., 2004; Schwartz, 1994; Stoeger et al., 2006). The secretion of inflammatory molecules, such as inflammatory cytokines and reactive oxygen species (ROS), is induced by various organic ions, organic chemicals, and polycyclic aromatic hydrocarbons, as well as by microorganisms, contained in fine dust (Kim et al., 2015). In the present study, the immunological characteristics of PMPS, a bacterium isolated from fine dust, were examined. PMPS induced the secretion of pro-inflammatory cytokines and chemokines in lung epithelial cells, lung alveolar macrophages, and macrophages through the activation of NF- $\kappa$ B and MAPK signaling pathways. Additionally, PMPS showed higher infectivity, pathogenicity, and

cytotoxicity to all the cells examined, including lung epithelial cells and macrophages than PS. In regards to investigating pathophysiology, using 3D constructs such as organoids and spheroids as disease models have distinct advantages over conventional 2D monolayer cultures as the former precisely reproduces the complexity and function of human tissues. Previous studies have examined the impact of PM<sub>2.5</sub> in 3D organoids, identifying that exposure to PM<sub>2.5</sub> has been shown to induce inflammation and apoptosis in alveolar and retinal organoid crypts (Kim et al., 2020; Zeng et al., 2021). In the present study, PMPS infection caused toxic effects to spheroids mimicking human bronchial epithelium, indicating that bacteria inhaled along with PM pose a considerable human health risk (Fig. 3).

Exposure to PM<sub>10</sub> reportedly induces the production of cytokines, such as IL-6 and TNF- $\alpha$ , by macrophages in a TLR4/Myd88-dependent manner (Shoenfelt et al., 2009). Likewise, we found that PMPS treatment induced the production of cytokines and chemokines by the cells in a TLR4-dependent manner. Moreover, PM<sub>10</sub> showed TLR2-mediated IL-8 production (Camatini et al., 2012; Shoenfelt et al., 2009), and TLR2 and TLR4 expression was highest in MLE-12 cells after PM<sub>10</sub> treatment (Herath et al., 2020). Furthermore, PM<sub>2.5</sub> reinforced inflammatory cytokine production through the activation of TLR5, promoting the activation of NF- $\kappa$ B via NOX4-ROS signaling (Ryu et al., 2019). Taken together, these findings suggest that PM activates TLR and that PMPS present in PM can induce TLR-mediated inflammatory responses which are prominent in regulating bacterial pathogenicity *in vivo*. Moreover, other microorganisms present in fine dust have been shown to activate inflammatory responses through TLR signaling (Becker et al., 2002; Shoenfelt et al., 2009). We observed that the inflammatory response

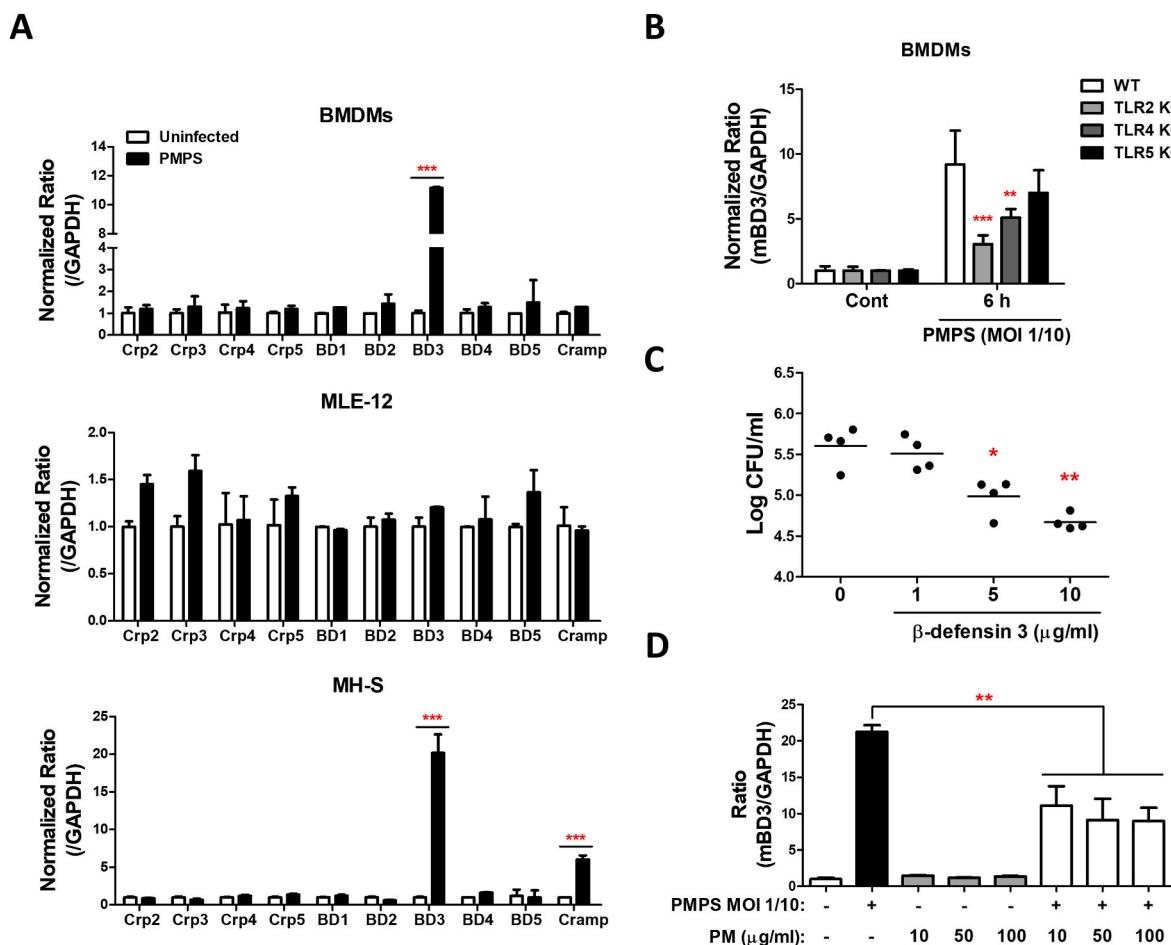


**Fig. 8.** PMPS induces TLR-dependent expression of BD3 and is inhibited by PM treatment. A and B. BMDMs, MLE-12 cells, and MH-S cells were infected with PMPS at MOIs of 1/10 and treated with gentamicin 1 h after infection. RNA was extracted from the cells 6 h after infection, and the expression of AMPs was determined using real-time qRT-PCR. Values shown are fold change relative to unstimulated cells, calculated from the average of two independent experiments. C. PMPS ( $1 \times 10^4$  CFU/ml) was incubated in LB broth at 37 °C in the presence or absence of recombinant BD3 (1, 5, and 10  $\mu$ g/ml). Culture broth were plated on LB agar and incubated overnight. D. BMDMs were infected with PMPS at an MOI of 1/10 and treated with gentamicin 1 h after infection, and total RNA was extracted 6 h after infection. Data were presented as the mean  $\pm$  SD of three independent experiments. \* $p < 0.05$ , \*\* $p < 0.01$ , and \*\*\* $p < 0.001$ .

induced by PMPS was mediated by TLR2 and TLR4 (Fig. 6). Intriguingly, overall cytokine and chemokine productions assessed 6 h post PMPS infection were reduced from TLR2- and TLR4-deficient BMDMs compared to WT, while TNF- $\alpha$  and MIP-1 $\alpha$  productions were rather increased in TLR4-deficient BMDM, unlike other cytokines and chemokines, when compared to the WT at 18 h post-infection. We assumed that such a result was due to the increased PMPS load in the lungs of TLR4-deficient mice due to uncontrolled bacterial amplification (Fig. 7). This was confirmed by an independent experiment using UV-killed PMPS, as the secretion of TNF- $\alpha$  and MIP-1 $\alpha$  from TLR-deficient BMDMs was comparable to WT at 18 h post-treatment (Data not shown). Yet, we believe further evaluations are required in regards to understanding the TLR4-mediated signaling pathways and how their deficiency in BMDM leads to increased production of cytokines in particular after PMPS infection.

Recently, it has been actively addressed that cell and tissue damage caused by PM intensifies bacterial infections. For instance, PM enhanced *P. aeruginosa* PAO1 infection by disrupting the airway epithelial barrier through oxidative stress and increasing IL-8 production PM-concentration-dependently (Chen et al., 2018; Liu et al., 2019). Additionally, PM inhibited macrophage phagocytosis by interfering with autophagy (Li et al., 2020), and increased *P. aeruginosa* PAO1 proliferation (Borcherding et al., 2013). Similarly, PM<sub>10</sub> increased PMPS-induced cytokine production in lung epithelial cells and

macrophages dependent on the PM concentration increased PMPS proliferation, and exacerbated PMPS-induced tissue damage in mice in the present study (Fig. 5). These results show that PM may increase the risk of bacterial infection and the pathogenicity of PMPS, despite that PMPS are not highly pathogenic.

AMPs are ubiquitous and serve as the first line of defense against invading microorganisms (Boman, 1995). The signaling mechanism of TLRs also regulates various immune responses and activates the expression of AMPs (Lee et al., 2019; Pasupuleti et al., 2012). Coal fly ash (CFA) treatment reduced AMP activity against *P. aeruginosa* PAO1 (Borcherding et al., 2013), while PM treatment suppressed *P. aeruginosa* PAO1-induced expression of hBD2 in BEAS-2B cells. In contrast, a study showed that although PM stimulated TLRs to activate signaling, it did not significantly induce AMP expression (Chen et al., 2018). In the present study, PM treatment reduced PMPS-induced expression of BD3 in MH-S cells and BMDMs.

The present study focused on the immunological properties of PMPS isolated from PM. Investigating the components of PM may help identify the causes of various diseases developed from PM inhalation. However, relatively little is known about the characteristics of bacteria present in this fine dust. In summary, the results of the present study showed that PMPS, present in PM, can deteriorate the risk of respiratory diseases. However, further studies are needed to elucidate the mechanism through which PM affects non-pathogenic bacteria, which are likely to

be responsible for PM-induced diseases.

## 5. Conclusion

In the present study, we demonstrated a previously unknown link between *P. stutzeri* present in particulate matter and the pathogenesis of lung damage in the infected host. PMPS induces a more severe inflammatory response, infectivity, and cytotoxicity than the comparative PS strain, leading to lung injury *in vivo*. Of note, in three-dimensional (3D) human airway spheroids mimicking human bronchial epithelium, *P. stutzeri* PM101005 (PMPS) produced more potent inflammatory cytokines than *P. stutzeri* (PS) ATCC17588. We also observed that PMPS induces an inflammatory response following NF- $\kappa$ B and MAPK activation via recognizing TLR2, TLR4, and TLR5 as host receptors. Furthermore, in the host cells infected with PMPS,  $\beta$ -defensin 3, expressed in a TLRs-dependent manner, showed a direct antibacterial effect on PMPS that may represent a therapeutic target to ameliorate PMPS-mediated pathogenesis. Consistent with the previous studies showing that PM exposure is associated with increased severity of bacterial infection, our results also support that PM increases the infectivity of PMPS. The results of this study are the first to elucidate the immunological characteristics of PMPS isolated from atmospheric particulate matter as a major air pollutant, suggesting a bacterial risk as one of the causes of lung damage from exposure to PM.

## Author Statement

**Yu-Jin Jeong:** Conception or design of the work; Data collection; Data Formal analysis and interpretation; Drafting the article; Critical revision of the article. **Chang-Ung Kim:** Conception or design of the work; Data collection; Data Formal analysis and interpretation; Drafting the article. **Kyung-Soo Lee:** Data collection; Data Formal analysis and interpretation. **Ji Hyung Kim:** Data collection; Data Formal analysis and interpretation. **Seo Young Park:** Data collection; Data Formal analysis and interpretation. **Ahn Young Jeong:** Data collection; Data Formal analysis and interpretation. **Jun Bong Lee:** Data collection; Data Formal analysis and conducting experiments with animals. **Doo-Jin Kim:** Data collection; Data Formal analysis and interpretation. **Young-Jun Park:** Data Formal analysis and interpretation. **Moo-Seung Lee:** Conceptualization or design of the work; Supervision; Writing –review & editing. All persons who meet authorship criteria are listed as authors, and all authors certify, that they have participated sufficiently in the work to take public responsibility for the content, including participation in the concept, design, analysis, writing, or revision of the manuscript.

## Declaration of competing interest

The authors declare that they have no known competing financial interests or personal relationships that could have appeared to influence the work reported in this paper.

## Data availability

Data will be made available on request.

## Acknowledgements

This work was supported by the KRIBB Research Initiative Program (KGM9942213, KGM5322214) and a grant from the National Research Foundation of Korea (NRF) funded by the Ministry of Science, ICT and Future Planning (2018M3A9H4077992, 2021M3A9H3016046) and by the Basic Science Research Program through the National Research Foundation of Korea (NRF) (2022R1A2C1003699) and also the “Cooperative Research Program for Agriculture Science and Technology Development (Project No. PJ015001022022)” Rural Development Administration, Republic of Korea.

## Appendix A. Supplementary data

Supplementary data to this article can be found online at <https://doi.org/10.1016/j.envpol.2022.120741>.

## References

- Arooj, M., Ali, I., Kang, H.K., Hyun, J.W., Koh, Y.S., 2020. Inhibitory effect of particulate matter on toll-like receptor 9 stimulated dendritic cells by downregulating mitogen-activated protein kinase and NF-kappaB pathway. *J. Toxicol. Environ. Health* 83, 341–350.
- Becker, S., Fenton, M.J., Soukup, J.M., 2002. Involvement of microbial components and toll-like receptors 2 and 4 in cytokine responses to air pollution particles. *Am. J. Respir. Cell Mol. Biol.* 27, 611–618.
- Boman, H.G., 1995. Peptide antibiotics and their role in innate immunity. *Annu. Rev. Immunol.* 13, 61–92.
- Borchering, J.A., Chen, H., Caraballo, J.C., Baltrusaitis, J., Pezzulo, A.A., Zabner, J., Grassian, V.H., Comellas, A.P., 2013. Coal fly ash impairs airway antimicrobial peptides and increases bacterial growth. *PLoS One* 8, e57673.
- Brook, R.D., Rajagopalan, S., Pope 3rd, C.A., Brook, J.R., Bhatnagar, A., Diez-Roux, A.V., Holguin, F., Hong, Y., Luepker, R.V., Mittleman, M.A., Peters, A., Siscovick, D., Smith Jr., S.C., Whitsett, L., Kaufman, J.D., 2010. American heart association council on, E., prevention, C.o.t.K.i.C.D., council on nutrition, P.A., metabolism. Particulate matter air pollution and cardiovascular disease: An update to the scientific statement from the American Heart Association. *Circulation* 121, 2331–2378.
- Budinger, G.R., McKell, J.L., Ulrich, D., Foiles, N., Weiss, I., Chiarella, S.E., Gonzalez, A., Soberanes, S., Ghio, A.J., Nigdelioglu, R., Mutlu, E.A., Radigan, K.A., Green, D., Kwaan, H.C., Mutlu, G.M., 2011. Particulate matter-induced lung inflammation increases systemic levels of PAI-1 and activates coagulation through distinct mechanisms. *PLoS One* 6, e18525.
- Camatini, M., Corvaja, V., Pezzolato, E., Mantecca, P., Gualtieri, M., 2012. PM10-biogenic fraction drives the seasonal variation of proinflammatory response in A549 cells. *Environ. Toxicol.* 27, 63–73.
- Cao, C., Jiang, W., Wang, B., Fang, J., Lang, J., Tian, G., Jiang, J., Zhu, T.F., 2014. Inhalable microorganisms in Beijing's PM2.5 and PM10 pollutants during a severe smog event. *Environ. Sci. Technol.* 48, 1499–1507.
- Celada, A., Gray, P.W., Rinderknecht, E., Schreiber, R.D., 1984. Evidence for a gamma-interferon receptor that regulates macrophage tumoricidal activity. *J. Exp. Med.* 160, 55–74.
- Chen, X., Liu, J., Zhou, J., Wang, J., Chen, C., Song, Y., Pan, J., 2018. Urban particulate matter (PM) suppresses airway antibacterial defence. *Respir. Res.* 19, 5.
- Cheng, M.H., Chiu, H.F., Yang, C.Y., 2015. Coarse particulate air pollution associated with increased risk of hospital admissions for respiratory diseases in a tropical city, kaohsiung, taiwan. *Int. J. Environ. Res. Publ. Health* 12, 13053–13068.
- Dajon, M., Iribarren, K., Cremer, I., 2017. Toll-like receptor stimulation in cancer: a pro- and anti-tumor double-edged sword. *Immunobiology* 222, 89–100.
- Eckle, T., Brodsky, K., Bonney, M., Packard, T., Han, J., Borchers, C.H., Mariani, T.J., Kominsky, D.J., Mittelbronn, M., Eltschig, H.K., 2013. HIF1A reduces acute lung injury by optimizing carbohydrate metabolism in the alveolar epithelium. *PLoS Biol.* 11, e1001665.
- Faure, E., Equils, O., Sieling, P.A., Thomas, L., Zhang, F.X., Kirschning, C.J., Polentarutti, N., Muzio, M., Arditi, M., 2000. Bacterial lipopolysaccharide activates NF-kappaB through toll-like receptor 4 (TLR-4) in cultured human dermal endothelial cells. Differential expression of TLR-4 and TLR-2 in endothelial cells. *J. Biol. Chem.* 275, 11058–11063.
- Goetz, A., Yu, V.L., Hanchett, J.E., Rihs, J.D., 1983. *Pseudomonas stutzeri* bacteremia associated with hemodialysis. *Arch. Intern. Med.* 143, 1909–1912.
- Grahame, T., Schlesinger, R., 2005. Evaluating the health risk from secondary sulfates in eastern North American regional ambient air particulate matter. *Inhal. Toxicol.* 17, 15–27.
- Guohua, F., Tiejuan, Z., Xinping, M., Juan, X., 2021. Melatonin protects against PM2.5-induced lung injury by inhibiting ferroptosis of lung epithelial cells in a Nrf2-dependent manner. *Ecotoxicol. Environ. Saf.* 223, 112588.
- Herath, K., Kim, H.J., Jang, J.H., Kim, H.S., Kim, H.J., Jeon, Y.J., Jee, Y., 2020. Mojabanchromanol isolated from sargassum horneri attenuates particulate matter induced inflammatory responses via suppressing TLR2/4/7-MAPK signaling in MLE-12 cells. *Mar. Drugs* 18.
- Heroux, M.E., Anderson, H.R., Atkinson, R., Brunekreef, B., Cohen, A., Forastiere, F., Hurley, F., Katsouyanni, K., Krewski, D., Krzyzanowski, M., Kunzli, N., Mills, I., Querol, X., Ostro, B., Walton, H., 2015. Quantifying the health impacts of ambient air pollutants: recommendations of a WHO/Europe project. *Int. J. Publ. Health* 60, 619–627.
- Jezierska, A., Kolosova, I.A., Verin, A.D., 2011. Toll like receptors signaling pathways as a target for therapeutic interventions. *Curr. Signal Transduct. Ther.* 6, 428–440.
- Johnson, G.B., Brunn, G.J., Platt, J.L., 2004. Cutting edge: an endogenous pathway to systemic inflammatory response syndrome (SIRS)-like reactions through Toll-like receptor 4. *J. Immunol.* 172, 20–24.
- Kalra, D., Sati, A., Shankar, S., Jha, A., 2015. Corneal infection by *Pseudomonas stutzeri* following excision of trigeminal nerve schwannoma. *BMJ Case Rep.* 2015, bcr2014207496.
- Kawasaki, T., Kawai, T., 2014. Toll-like receptor signaling pathways. *Front. Immunol.* 5, 461.
- Kim, J.H., Kim, J., Kim, W.J., Choi, Y.H., Yang, S.R., Hong, S.H., 2020. Diesel particulate matter 2.5 induces epithelial-to-mesenchymal transition and upregulation of SARS-

- CoV-2 receptor during human pluripotent stem cell-derived alveolar organoid development. *Int. J. Environ. Res. Publ. Health* 17.
- Kim, K.H., Kabir, E., Kabir, S., 2015. A review on the human health impact of airborne particulate matter. *Environ. Int.* 74, 136–143.
- Kumar, S., Stecher, G., Tamura, K., 2016. MEGA7: molecular evolutionary genetics analysis version 7.0 for bigger datasets. *Mol. Biol. Evol.* 33, 1870–1874.
- Lalucat, J., Bennisar, A., Bosch, R., Garcia-Valdes, E., Palleroni, N.J., 2006. Biology of *Pseudomonas stutzeri*. *Microbiol. Mol. Biol. Rev.* 70, 510–547.
- Lee, E.Y., Lee, M.W., Wong, G.C.L., 2019. Modulation of toll-like receptor signaling by antimicrobial peptides. *Semin. Cell Dev. Biol.* 88, 173–184.
- Li, N., Hao, M., Phalen, R.F., Hinds, W.C., Nel, A.E., 2003. Particulate air pollutants and asthma. A paradigm for the role of oxidative stress in PM-induced adverse health effects. *Clin. Immunol.* 109, 250–265.
- Li, N., Wang, M., Oberley, T.D., Sempf, J.M., Nel, A.E., 2002. Comparison of the pro-oxidative and proinflammatory effects of organic diesel exhaust particle chemicals in bronchial epithelial cells and macrophages. *J. Immunol.* 169, 4531–4541.
- Li, Y., Yong, Y.L., Yang, M., Wang, W., Qu, X., Dang, X., Shang, D., Shao, Y., Liu, J., Chang, Y., 2020. Fine particulate matter inhibits phagocytosis of macrophages by disturbing autophagy. *Faseb. J.* 34, 16716–16735.
- Liu, J., Chen, X., Dou, M., He, H., Ju, M., Ji, S., Zhou, J., Chen, C., Zhang, D., Miao, C., Song, Y., 2019. Particulate matter disrupts airway epithelial barrier via oxidative stress to promote *Pseudomonas aeruginosa* infection. *J. Thorac. Dis.* 11, 2617–2627.
- Medina-Ramon, M., Zanobetti, A., Schwartz, J., 2006. The effect of ozone and PM10 on hospital admissions for pneumonia and chronic obstructive pulmonary disease: a national multicity study. *Am. J. Epidemiol.* 163, 579–588.
- Meissner, N.N., Swain, S., Tighe, M., Harmsen, A., Harmsen, A., 2005. Role of type I IFNs in pulmonary complications of *Pneumocystis murina* infection. *J. Immunol.* 174, 5462–5471.
- Mushtaq, N., Ezzati, M., Hall, L., Dickson, I., Kirwan, M., Png, K.M., Mudway, I.S., Grigg, J., 2011. Adhesion of *Streptococcus pneumoniae* to human airway epithelial cells exposed to urban particulate matter. *J. Allergy Clin. Immunol.* 127, 1236–1242 e1232.
- Neri, T., Pergoli, L., Petrini, S., Gravendonk, L., Balia, C., Scalise, V., Amoroso, A., Pedrinelli, R., Paggiaro, P., Bollati, V., Celi, A., 2016. Particulate matter induces prothrombotic microparticle shedding by human mononuclear and endothelial cells. *Toxicol. Vitro* 32, 333–338.
- Noble, R.C., Overman, S.B., 1994. *Pseudomonas stutzeri* infection. A review of hospital isolates and a review of the literature. *Diagn. Microbiol. Infect. Dis.* 19, 51–56.
- Nozza, E., Valentini, S., Melzi, G., Vecchi, R., Corsini, E., 2021. Advances on the immunotoxicity of outdoor particulate matter: a focus on physical and chemical properties and respiratory defence mechanisms. *Sci. Total Environ.* 780, 146391.
- Pasupuleti, M., Schmidtchen, A., Malmsten, M., 2012. Antimicrobial peptides: key components of the innate immune system. *Crit. Rev. Biotechnol.* 32, 143–171.
- Piaścik, M., Perez Przyk, E., Held, A., 2019. The Certification of the Mass Fractions of Selected Polycyclic Aromatic Hydrocarbons (PAHs) in Fine Dust (PM10-like Matrix). European Commission, Joint Research Centre Institute for Reference Materials and Measurements (IRMM), Geel (BE).
- Priyamvada, H., Singh, R.K., Akila, M., Ravikrishna, R., Verma, R.S., Gunthe, S.S., 2017. Seasonal variation of the dominant allergenic fungal aerosols - one year study from southern Indian region. *Sci. Rep.* 7, 11171.
- Qin, N., Liang, P., Wu, C., Wang, G., Xu, Q., Xiong, X., Wang, T., Zolfo, M., Segata, N., Qin, H., Knight, R., Gilbert, J.A., Zhu, T.F., 2020. Longitudinal survey of microbiome associated with particulate matter in a megacity. *Genome Biol.* 21, 55.
- Ryu, Y.S., Kang, K.A., Piao, M.J., Ahn, M.J., Yi, J.M., Hyun, Y.M., Kim, S.H., Ko, M.K., Park, C.O., Hyun, J.W., 2019. Particulate matter induces inflammatory cytokine production via activation of NFκB by TLR5-NOX4-ROS signaling in human skin keratinocyte and mouse skin. *Redox Biol.* 21, 101080.
- Saitoh, S., Miyake, K., 2009. Regulatory molecules required for nucleotide-sensing Toll-like receptors. *Immunol. Rev.* 227, 32–43.
- Schaumann, F., Borm, P.J., Herbrich, A., Knoch, J., Pitz, M., Schins, R.P., Luetting, B., Hohlfeld, J.M., Heinrich, J., Krug, N., 2004. Metal-rich ambient particles (particulate matter 2.5) cause airway inflammation in healthy subjects. *Am. J. Respir. Crit. Care Med.* 170, 898–903.
- Schlesinger, R.B., Cassee, F., 2003. Atmospheric secondary inorganic particulate matter: the toxicological perspective as a basis for health effects risk assessment. *Inhal. Toxicol.* 15, 197–235.
- Schwartz, J., 1994. Air pollution and daily mortality: a review and meta analysis. *Environ. Res.* 64, 36–52.
- Shoenfelt, J., Mitkus, R.J., Zeisler, R., Spatz, R.O., Powell, J., Fenton, M.J., Squibb, K.A., Medvedev, A.E., 2009. Involvement of TLR2 and TLR4 in inflammatory immune responses induced by fine and coarse ambient air particulate matter. *J. Leukoc. Biol.* 86, 303–312.
- Stoeger, T., Reinhard, C., Takenaka, S., Schroepel, A., Karg, E., Ritter, B., Heyder, J., Schulz, H., 2006. Instillation of six different ultrafine carbon particles indicates a surface area threshold dose for acute lung inflammation in mice. *Environ. Health Perspect.* 114, 328–333.
- Tarin-Carrasco, P., Im, U., Geels, C., Palacios-Pena, L., Jimenez-Guerrero, P., 2021. Contribution of fine particulate matter to present and future premature mortality over Europe: a non-linear response. *Environ. Int.* 153, 106517.
- Woodward, N.C., Levine, M.C., Haghani, A., Shirmohammadi, F., Saffari, A., Sioutas, C., Morgan, T.E., Finch, C.E., 2017. Toll-like receptor 4 in glial inflammatory responses to air pollution in vitro and in vivo. *J. Neuroinflammation* 14, 84.
- Yan, D., Zhang, T., Su, J., Zhao, L.L., Wang, H., Fang, X.M., Zhang, Y.Q., Liu, H.Y., Yu, L.Y., 2018. Structural variation in the bacterial community associated with airborne particulate matter in Beijing, China, during hazy and nonhazy days. *Appl. Environ. Microbiol.* 84.
- Yang, H.S., Sim, H.J., Cho, H., Bang, W.Y., Kim, H.E., Kwon, T.K., Kwon, T., Park, T.J., 2020. Alpha-tocopherol exerts protective function against the mucotoxicity of particulate matter in amphibian and human goblet cells. *Sci. Rep.* 10, 6224.
- Zeng, Y., Li, M., Zou, T., Chen, X., Li, Q., Li, Y., Ge, L., Chen, S., Xu, H., 2021. The impact of particulate matter (PM2.5) on human retinal development in hESC-derived retinal organoids. *Front. Cell Dev. Biol.* 9, 607341.
- Zhi, Y., Chen, X., Cao, G., Chen, F., Seo, H.S., Li, F., 2022. The effects of air pollutants exposure on the transmission and severity of invasive infection caused by an opportunistic pathogen *Streptococcus pyogenes*. *Environ. Pollut.* 310, 119826.